The EMBO Journal (2010) 29, 619–631 | © 2010 European Molecular Biology Organization | All Rights Reserved 0261-4189/10
www.embojournal.org

THE EMBO JOURNAL

The IKK complex contributes to the induction of autophagy

Alfredo Criollo[1,2,3,4], Laura Senovilla[1,2,3], Hélène Authier[5], Maria Chiara Maiuri[1,2,3,6], Eugenia Morselli[1,2,3], Ilio Vitale[1,2,3], Oliver Kepp[1,2,3], Ezgi Tasdemir[1,2,3], Lorenzo Galluzzi[1,2,3], Shensi Shen[1,2,3], Maximilien Tailler[1,2,3], Nicolas Delahaye[2,3,7], Antoine Tesniere[1,2,3], Daniela De Stefano[6], Aména Ben Younes[1,2,3], Francis Harper[8], Gérard Pierron[8], Sergio Lavandero[4], Laurence Zitvogel[2,3,7], Alain Israel[9], Véronique Baud[5] and Guido Kroemer[1,2,3,*]

[1]INSERM, U848, Villejuif, France, [2]Institut Gustave Roussy, Villejuif, France, [3]Université Paris Sud–Paris 11, Villejuif, France, [4]Faculty of Chemical and Pharmaceutical Sciences/Medicine, FONDAP Center CEMC, University of Chile, Santiago, Chile, [5]Institut Cochin, Université Paris Descartes, CNRS (UMR 8104), Paris, France, [6]Dipartimento di Farmacologia Sperimentale, Università degli Studi di Napoli, Napoli, Italy, [7]INSERM, U805, Villejuif, France, [8]CNRS, FRE 2937, Institut Andre Lwoff, Villejuif, France and [9]CNRS URA 2582, Institut Pasteur, Paris, France

In response to stress, cells start transcriptional and transcription-independent programs that can lead to adaptation or death. Here, we show that multiple inducers of autophagy, including nutrient depletion, trigger the activation of the IKK (IκB kinase) complex that is best known for its essential role in the activation of the transcription factor NF-κB by stress. Constitutively active IKK subunits stimulated autophagy and transduced multiple signals that operate in starvation-induced autophagy, including the phosphorylation of AMPK and JNK1. Genetic inhibition of the nuclear translocation of NF-κB or ablation of the p65/RelA NF-κB subunit failed to suppress IKK-induced autophagy, indicating that IKK can promote the autophagic pathway in an NF-κB-independent manner. In murine and human cells, knockout and/or knockdown of IKK subunits (but not that of p65) prevented the induction of autophagy in response to multiple stimuli. Moreover, the knockout of IKK-β suppressed the activation of autophagy by food deprivation or rapamycin injections *in vivo*, in mice. Altogether, these results indicate that IKK has a cardinal role in the stimulation of autophagy by physiological and pharmacological stimuli.

The EMBO Journal (2010) **29,** 619–631. doi:10.1038/emboj.2009.364; Published online 3 December 2009
Subject Categories: signal transduction; cellular metabolism
Keywords: hypoxia; mice; NF-κB; rapamycin; starvation

*Corresponding author. INSERM, U848, Institut Gustave Roussy, PR1 39, rue Camille Desmoulins, Villejuif F-94805, France.
Tel. +33 1 4211 6046; Fax: +33 1 4211 6047;
E-mail: kroemer@orange.fr

Received: 18 August 2009; accepted: 6 November 2009; published online: 3 December 2009

Introduction

In response to sub-lethal stress, cells mount responses that allow them to repair damage and to adapt to the changing environment. Such adaptive responses include immediate cytoplasmic alterations that do not require transcriptional reprogramming and that generate specific sub-cellular structures, such as stress granules (Anderson and Kedersha, 2008; which allow cells to store and eliminate stalled translation pre-initiation complexes) and autophagosomes (Klionsky, 2004; which allow cells to eliminate damaged organelles and to mobilize energy reserves). Autophagosomes are double-membraned vesicles that mediate the first step of macroautophagy (hitherto referred to as 'autophagy') by sequestering organelles, long-lived proteins and/or portions of the cytoplasm. Autophagosomes mature by fusing with lysosomes (thereby becoming so-called 'autolysosomes'), which leads to the degradation of their luminal content (Klionsky, 2004; Levine and Kroemer, 2008). Although systematic studies of different manifestations of cytoplasmic stress responses are lacking, these may have common denominators, such as the phosphorylation-dependent inactivation of the translation initiation factor eIF2α, an event that is required for both the generation of stress granules and autophagy (Kedersha *et al*, 2002; Talloczy *et al*, 2002).

Adaptation to stress frequently involves transcriptional programs such as those orchestrated by p53 after DNA damage (Riley *et al*, 2008), heat shock transcription factors (HSFs) on heat shock (Anckar and Sistonen, 2007), hypoxia-inducible factor 1 (HIF-1) in conditions of oxygen shortage (Semenza, 2007), and NF-κB in response to a wide array of stimuli (Baud and Karin, 2009). The NF-κB dimers are normally sequestered in the cytoplasm through interaction with inhibitory IκB proteins. Multiple external stimuli lead to the phosphorylation of IκB, thereby targeting it to ubiquitination and consequent proteasome-mediated destruction. The degradation of IκB enables NF-κB dimers to translocate to the nucleus, where they transactivate several target genes, many of which inhibit apoptosis, trigger cell cycle progression and stimulate inflammation. The IκB kinase (IKK) complex is composed by two highly homologous catalytic kinase subunits (IKKα and IKKβ) and a regulatory subunit (IKKγ, also termed NEMO; Hacker and Karin, 2006). The IKK complex can be activated by upstream kinases that connect it to signals that emanate from death receptors of the TNF family, pattern-recognition receptors of the toll-like receptor (TLR) family or DNA damage (Hacker and Karin, 2006; Perkins, 2007; Baud and Karin, 2009; Vallabhapurapu and Karin, 2009).

Controversial information is available on the crosstalk between transcriptional and cytoplasmic responses to stress. Hypoxia can induce autophagy through the HIF-1-mediated transactivation of proteins such as BNIP3 (Zhang *et al*, 2008), but may also act in an HIF-1- and BNIP3-independent manner (Papandreou *et al*, 2008). p53 can elicit the transcription of

autophagic inducers such as DRAM and SESN2 (Crighton *et al*, 2006; Budanov and Karin, 2008), yet can repress autophagy at the cytoplasmic level through a transcription-independent mechanism (Tasdemir *et al*, 2008). The putative links between autophagy and NF-κB, which is perhaps the transcription factor most frequently activated by stress, (Perkins, 2007; Baud and Karin, 2009; Vallabhapurapu and Karin, 2009) are also a matter of debate. According to some studies, NF-κB can induce autophagy by transactivating the autophagy-triggering protein Beclin-1 (Copetti *et al*, 2009). However, NF-κB has also been reported to inhibit autophagy, for instance in the context of TNFα-induced cell death (Djavaheri-Mergny *et al*, 2006) or in macrophages infected by enterobacteria (Schlottmann *et al*, 2008). Insulin- or TNFα-induced activation of IKKα or IKKβ has been implicated in the phosphorylation of tuberous sclerosis complex 1/2 (TSC1/2), resulting in activation of mTOR and inhibition of autophagy (Lee *et al*, 2007; Dan and Baldwin, 2008). Moreover, autophagy might itself contribute to the inhibition of the NF-κB pathway. Thus, autophagy has been shown to mediate the degradation of the three subunits (α, β and γ) of the IKK complex and of its upstream activator NF-κB-inducing kinase (NIK; Qing *et al*, 2007). Moreover, autophagy mediates the specific depletion of p62 (also known as sequestosome 1), which is involved in the activation of the IKK complex (Martin *et al*, 2006; Duran *et al*, 2008).

On the basis of these uncertainties and the results from an unbiased screen revealing IKK as a putative regulator of autophagy (see below), we decided to investigate the possible links between the NF-κB activation pathway and autophagy. Here, we report the finding that IKK activation is sufficient to promote autophagy though an NF-κB-independent mechanism, and that IKK is required for optimal autophagy induction.

Results and discussion

Autophagic stimuli can activate IKK without stimulating NF-κB

Twenty among the 482 agents contained in the ICCB library were able to reduce the starvation-induced redistribution of the autophagosome marker GFP–LC3 into cytoplasmic puncta (a macroautophagy-specific process that does not occur during chaperone-mediated autophagy) by more than 65%, in osteosarcoma U2OS cells (Figure 1A). Among these twenty agents, three are known to inhibit IKK: BAY 11-7082 as a direct kinase inhibitor, as well as geldanamycin and its 17-allylamino-derivative as inhibitors of HSP90, which is obligatory for IKK activation (Broemer *et al*, 2004). Driven by these results, we investigated the possible contribution of IKK to autophagy. In response to the most physiological inducer of autophagy, nutrient starvation (Mizushima and Klionsky, 2007), human cervical carcinoma HeLa cells exhibited the phosphorylation of IKKα/β on serines 177/181 and of IKKγ/NEMO on serine 376 (Figure 1B). The same occurred upon the induction of autophagy with the mTOR inhibitor rapamycin (Figure 1C), the p53 inhibitor pifithrin-α (Figure 1D), the ER stressor tunicamycin or the inositol monophosphatase inhibitor lithium (data not shown). Immunoprecipitated IKK complex exhibited an increased capacity to phosphorylate a semi-synthetic IκBα-derived substrate *in vitro* (Figure 1E–G). While the activation of autophagy by starvation, rapamycin or pifithrin-α induced a minor degree of phosphorylation of IκB (minor as compared with the positive control, TNF-α), autophagy failed to stimulate a detectable reduction in the abundance of IκB or to induce the nuclear translocation of NF-κB, as determined by EMSA (Figure 1H–J), or immunofluorescence detection of the NF-κB subunit p65/RelA (Supplementary Figure S1). Accordingly, in HeLa cells, autophagy-inducing conditions did not result in the transactivation of quintessential NF-κB target genes, such as *TNF-α*, *IL-6*, *IL-8* and *CCL-2*, which were induced by the NF-κB activator TNF-α (Supplementary Figure S2). In line with these observations, non-small cell lung cancer (NSCLC) A549 cells failed to translocate a GFP–p65 fusion protein into the nucleus as they were exposed to autophagic stimuli (Supplementary Figure S3). In these cells, TNFα, which was used as a positive control for NF-κB activation (Djavaheri-Mergny *et al*, 2006), induced GFP–p65 nuclear translocation (Supplementary Figure S3), but failed to induce autophagy (data not shown). This suggests that TNFα stimulates a yet elusive autophagy-inhibitory signal (Djavaheri-Mergny *et al*, 2006). Finally, mouse embryonic fibroblasts (MEFs) exposed to various autophagy inducers manifested a minor activation of NF-κB (as compared with that observed on the administration of TNFα), mainly p65–p50 heterodimers, correlating with the degradation of IκB (Supplementary Figure S4). Altogether, these results indicate that autophagy induction correlates with IKK activation and IκB degradation but not necessarily with the activation of NF-κB.

IKK stimulates autophagy in an NF-κB-independent manner

Transfection with a constitutively active (CA) IKKβ mutant (due to two phosphomimetic point mutations of two serines in the activation loop, S177E and S181E; Mercurio *et al*, 1997) or with a NEMO variant (MN-NEMO) that constitutively activates the IKK complex (due to the introduction of an N-terminal myristoylation site that targets NEMO to the plasma membrane; Weil *et al*, 2003) caused several manifestations of autophagy. These included the aggregation of a GFP–LC3 fusion protein into cytoplasmic dots (Figure 2A and B), which correlates with LC3 lipidation (further corroborated by immunoblotting; Figure 2C), as well as the degradation of the protein p62, which is a selective substrate of autophagy (Klionsky *et al*, 2008; Figure 2A and C). Blockade of the IKK enzymatic activity (with the chemical inhibitor BAY11-7082) prevented autophagy induction by both CA-IKKβ and MN-NEMO (Figure 2B). Enhanced GFP–LC3 aggregation in cytoplasmic dots was observed in HeLa cells (Figure 2), as well as in six other human or murine cell lines (data not shown) transfected with CA-IKKβ or MN-NEMO. Theoretically, the accumulation of autophagosomes may reflect increased autophagic sequestration or decreased removal of autophagosomes by fusion with lysosomes (Klionsky *et al*, 2008; Levine and Kroemer, 2008). In conditions in which the lysosomal inhibitor bafilomycin A1 (BafA1) efficiently inhibited the fusion of lysosomes and autophagosomes (Supplementary Figure S5A and B), CA-IKKβ and MN-NEMO continued to increase the % of cells characterized by GFP–LC3 aggregation (Supplementary Figure S5C), indicating that IKK activation indeed stimulated autophagic sequestration. Transmission electron microscopy

A

Agent	% Inhibition of autophagy	Agent	% Inhibition of autophagy
Ro 31-8220	98.4±1.4	Hinokitiol	70.5±7.6
Triptolide	92.9±5.2	Geldanamycin	70.7±8.5
Lycorine	82.5±7.5	SB 203580	69.7±1.8
5-Iodotubercidin	82.5±1.6	Juglone	69.6±6.3
17-Allylamino-geldanamycin	79.5±2,7	Lavendustin A	68.9±9.0
Calphostin C	78.4±7,3	Deprenyl	68.5±0.4
Bay 11-7082	74.7±5.9	GF-109203X	68.3±7.2
IAA-94	74.0±7.1	Thalidomide	68.2±1.1
OBAA	73.5±7.0	Indirubin-3'-monoxime	68.0±6.1
Splitomycin	73.1±9.3	AG213 (Tyrphostin 47)	65.0±9.8

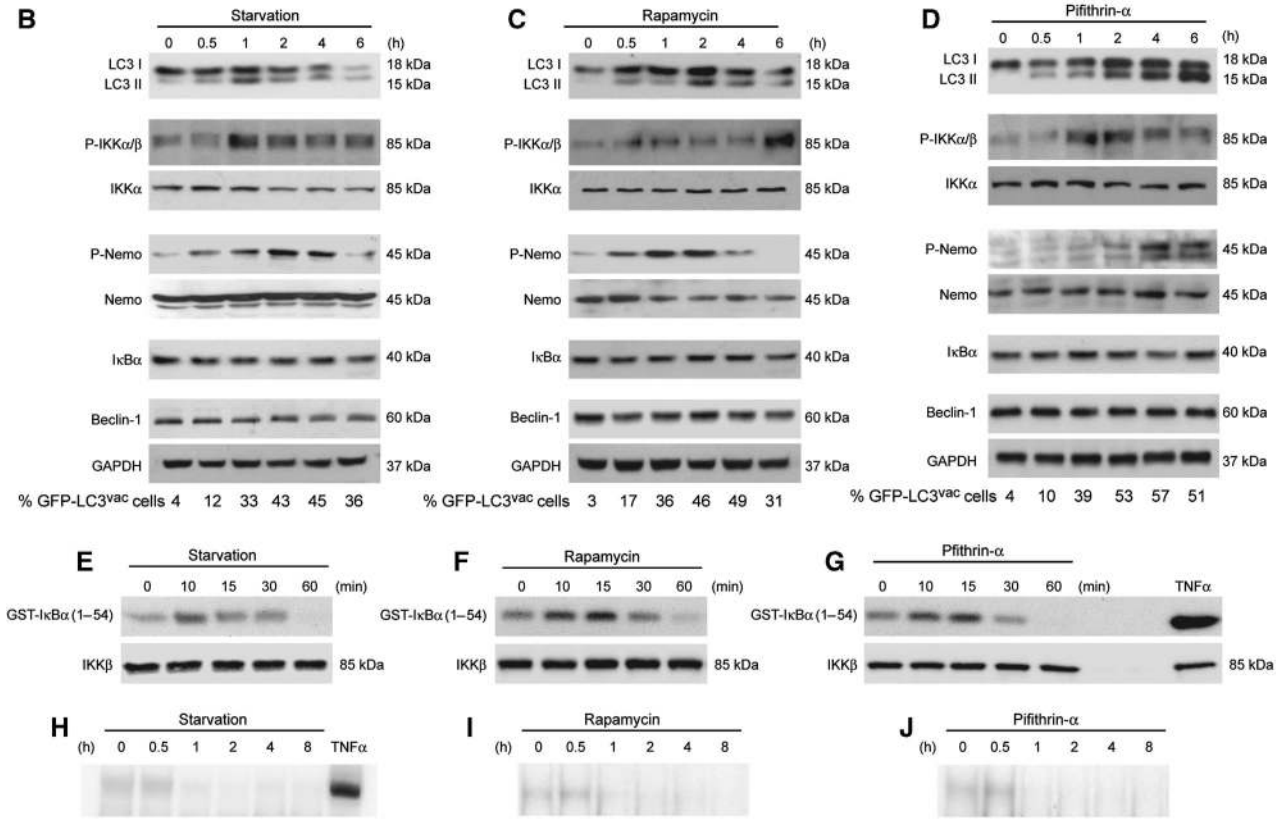

Figure 1 Impact of autophagy inducers on the NF-κB activation pathway. (**A**) Identification of IKK inhibitors as autophagy inhibitors in an unbiased screen. Levels of autophagy inhibition of ICCB compounds on nutrient deprivation in U2OS cells stably expressing GFP–LC3 and RFP–H2B were measured at 12 h after compound addition as described in Material and methods section (**B**–**D**). Effects of (**B**) starvation, (**C**) rapamycin or (**D**) pifithrin-α on IκBα levels and the phosphorylation status of the IKK complex. HeLa cells were exposed to autophagy inducers for the indicated time, followed by immunoblotting for the determination of the indicated proteins. The percentage values illustrate the fraction of cells that manifested a punctuated distribution of GFP–LC3 (% GFP–LC3^{vac} cells) after addition of the indicated agents, as assessed by immunofluorescence microscopy. (**E**–**G**) Determination of the enzymatic activity of the IKK complex. HeLa cells treated as in (**B**–**D**) were subjected to lysis and immunoprecipitation with an anti-NEMO antibody. Immunoprecipitates were tested for their capacity to phosphorylate *in vitro* a semi-synthetic derivative of IκBα, GST–IκBα (1–54). Lysates from cells treated with TNFα for 15 min were used as positive controls for IKK (and NF-κB activation). (**H**–**J**) NF-κB activation status. EMSA was used to determine the DNA-binding ability of NF-κB in cells treated as in (**B**–**D**). Results are representative of three independent experiments.

(TEM) corroborated the presence of double-membraned autophagosomes and single-membraned autolysosomes in HeLa cells expressing CA-IKKβ or MN-NEMO (Figure 2D and E). The autophagy-inducing effects of CA-IKKβ and MN-NEMO were significantly stronger than those of their unmodified counterparts, IKKβ and NEMO, respectively (Figure 2B–F). Constitutively active IKKβ and MN-NEMO distributed diffusely and to the plasma membrane, respectively, without any prominent co-localization with GFP–LC3 puncta (Supplementary Figure S6). Knockdown of essential proteins of the autophagic machinery (i.e. Atg10, Atg12, Beclin-1 and Vps34) abolished the increased GFP–LC3 aggregation triggered by CA-IKKβ or MN-NEMO (Figure 2F), confirming that this phenomenon reflects *bona fide* autophagy.

Next, we investigated whether the induction of autophagy by CA-IKKβ or MN-NEMO would be influenced by co-transfection with the IκB 'superrepressor' (IκSR) (DiDonato *et al*, 1995), a non-phosphorylatable IκB variant (due to the double

mutation S32A/S36A) that efficiently inhibits the IKK-induced nuclear translocation of p65/RelA (Figure 3A and B). IκSR failed to suppress autophagy induced by CA-IKKβ or MN-NEMO (Figure 3A, C, D and F). Accordingly, *p65*$^{-/-}$ NIH-3T3 fibroblasts activated autophagy comparably to their wild-type (WT) counterparts in response to multiple autophagy inducers, including starvation (Figure 3E), chemical stimuli (Supplementary Figure S7), CA-IKKβ and MN-NEMO

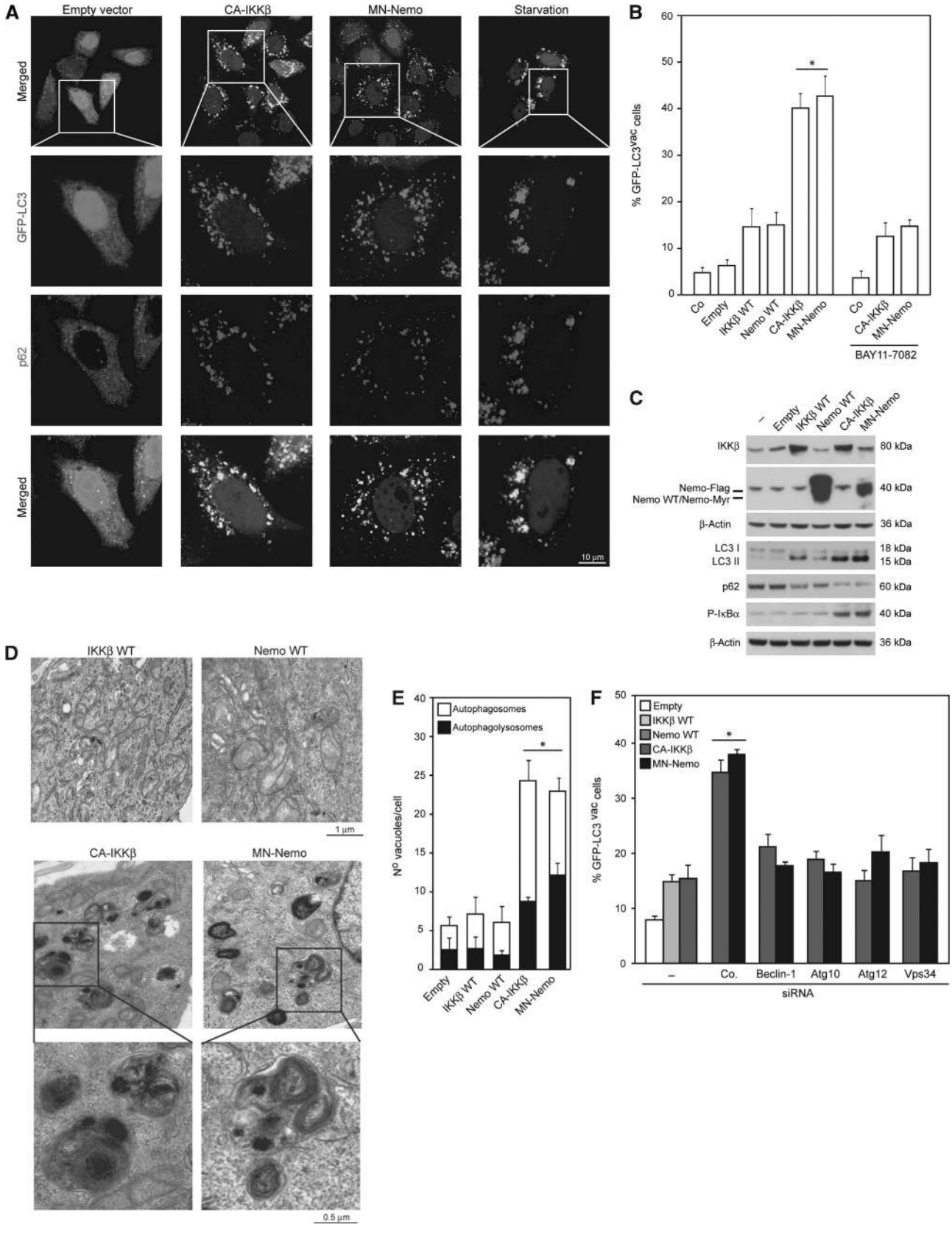

(Figure 3F). Furthermore, in NIH-3T3 cells, IκSR failed to prevent the induction of autophagy by CA-IKKβ or MN-NEMO (Figure 3F). Collectively, these results indicate that IKK can promote autophagy through a mechanism that does not involve NF-κB.

IKK stimulates canonical autophagy

Starvation-induced autophagy is strictly connected to the activation of AMP-activated kinase (AMPK) (Meley *et al*, 2006), the inhibition of mTOR (Mizushima and Klionsky, 2007), the degradation of cytoplasmic p53 (Tasdemir *et al*, 2008) and the dissociation of Beclin-1 from its inhibitory interaction with Bcl-2 (Pattingre *et al*, 2005; Wei *et al*, 2008). Induction of autophagy by starvation, as well as CA-IKKβ or MN-NEMO expression caused the hyperphosphorylation-dependent activation of AMPK, hypophosphorylation of the mTOR substrate $p70^{S6K}$ (which indicates mTOR inhibition), the depletion of p53 protein, as well as a reduction in the quantity of Beclin-1 that co-immunoprecipitated with Bcl-2 (Figure 4A and C). Autophagy induction by CA-IKKβ or MN-NEMO was prevented by the knockdown of the α-subunit of AMPK, and could not be further enhanced by rapamycin (Figure 4B), suggesting that IKK-stimulated autophagy is indeed controlled by the canonical AMPK/mTOR pathway. Both siRNA-mediated and pharmacological inhibition of MDM2 (the ubiquitin transferase that targets p53 to degradation) suppressed IKK-induced autophagy and at the same time prevented p53 degradation (Figure 4C), supporting the idea that p53 depletion is required for IKK-induced autophagy. To gain further insights into the mechanisms through which IKK induces autophagy, we performed an unbiased screen for serine/threonine kinase substrates that would be phosphorylated by cytosolic extracts from cells transfected with CA-IKKβ and MN-NEMO (Figure 4D). We observed that CA-IKKβ, MN-NEMO and other autophagy inducers (i.e. starvation, rapamycin and pifithrin-α) led to the generation of an enzymatic activity that phosphorylated a synthetic JNK1 substrate on serine/threonine residues (Figure 4D and E). Accordingly, CA-IKKβ- and MN-NEMO-transfected cells manifested the activating phosphorylation of JNK1 (Figure 4F). Moreover, both siRNA-mediated and pharmacological inhibition of JNK1 suppressed the induction of autophagy by CA-IKKβ or MN-NEMO (Figure 4G and H). Knockdown of the obligate JNK1 activators MKK4 and MKK7 (Lawler *et al*, 1998) also abolished autophagy induction by CA-IKKβ or MN-NEMO, whereas knockdown of c-Jun had no effect (Figure 4H and Supplementary Figure S8). Altogether, these results suggest that IKK alleviates the inhibition of autophagy normally ensured by p53 and mTOR, thereby promoting autophagy through AMPK and JNK1.

Contribution of endogenous IKK to autophagy

The aforementioned experiments indicate that constitutive activation of IKK suffices, but not that IKK is required, for the induction of autophagy. In MEFs, the knockout of the genes coding for IKKα, IKKβ, IKKγ/NEMO or for their upstream activator TAK1 (Hacker and Karin, 2006; Herrero-Martin *et al*, 2009) reduced (but did not abolish) autophagy induction by nutrient depletion or by treatment with rapamycin, pifithrin-α, lithium and tunicamycin (Figure 5A). Comparable results were obtained in HeLa cells when the same proteins were downregulated by specific siRNAs (Figure 5B). In these conditions, the knockout or knockdown of p65/RelA did not affect the autophagic response (Figure 5A and B). In MEFs, the absence of IKK subunits or that of autophagy-related proteins did not result into a major induction of cell death 24 h after the activation of autophagy by starvation, rapamycin, pifithrin-α, lithium and tunicamycin (Supplementary Figure S9A). However, genetic manipulations of the IKK complex as well as of the autophagic machinery (alone and in combination) sensitized MEFs to the lethal effect of prolonged (48 h) metabolic stress resulting from glucose deprivation and hypoxia (Figure 5C and D). These results indicate that the IKK complex subunits are required for optimal autophagy induction, at least *in vitro*, in cell lines.

To evaluate the contribution of the IKK complex to autophagy *in vivo*, we investigated the liver-specific conditional knockout of the gene coding for IKKβ (mediated by the Cre recombinase expressed under the control of the albumin promoter; Arkan *et al*, 2005). In response to the intraperitoneal injection of rapamycin or to 24 h of food deprivation, hepatocytes from control ($IKK\beta^{+/+}$: Cre_{Alb}) mice manifested the aggregation of LC3 in cytoplasmic dots, as determined by immunohistochemistry (Figure 6A–C). In contrast, livers from $IKK\beta^{\Delta hep}$ ($IKK\beta^{flox/flox}$: Cre_{Alb}) mice exhibited a strong reduction in rapamycin or starvation-induced LC3 aggregation (Figure 6A–C). Similar results were observed when autophagy was monitored by TEM (accumulation of autophagosomes and autolysosomes; Figure 6B) and by immunoblotting (LC3 maturation; Figure 6D). This autophagy-inhibitory effect was specific, as it could be detected in the liver from $IKK\beta^{\Delta hep}$ mice, but not in other organs (which express normal levels of IKKβ; Figure 6C, Supplementary Figures S10 and S11). Starvation led to massive autophagy induction in both the liver and spleen from control mice, but caused nuclear p65/RelA translocation only in hepatocytes

Figure 2 Activation of autophagy by IKK. (**A**, **B**) Induction of GFP–LC3 aggregation by CA-IKKβ or MN-NEMO. Human cervical carcinoma HeLa cells were co-transfected for 12 h with a GFP–LC3-encoding plasmid plus the pcDNA3.1 vector or constructs for the overexpression of wild type (WT) IKKβ, CA-IKKβ, WT NEMO or MN-NEMO, followed by immunofluorescence microscopy assessments of p62 expression. When indicated, the IKK inhibitor BAY11-7082 was added during the last 6 h of the experiment. In (**A**), representative immunofluorescence microphotographs are shown. The percentage of cells with GFP–LC3 puncta (% $GFP–LC3^{vac}$ cells) is reported in (**B**) (mean ± s.e.m., $n=3$, $^*P<0.05$). (**C**) Maturation of LC3 and depletion of p62 determined by immunoblotting. HeLa cells were transfected with the pcDNA3.1 vector or with IKKβ-, CA-IKKβ-, NEMO- or MN-NEMO-encoding plasmids (with a transfection efficiency of ∼70%) for 12 h, then processed for immunoblotting as described in Materials and methods section. (**D**, **E**) Transmission electron microscopy detection of autophagic vacuoles. HeLa cells were transfected as in (**C**) and then processed for transmission electron microscopy. Representative images are shown in (**D**) and the number of autophagosomes (white columns) and autophagolysosomes (black columns) per cell (mean ± s.e.m., $n=30$–40 cells, $^*P<0.05$) is depicted in (**E**). (**F**) Requirement of autophagy-relevant proteins for GFP–LC3 aggregation induced by CA-IKKβ or MN-NEMO. HeLa cells were transfected with a control siRNA (Co.) or with siRNAs targeting the indicated autophagy-relevant proteins for 24 h, and then with a GFP–LC3-endoding plasmid plus the indicated IKK-relevant constructs for additional 12 h, followed by immunofluorescence microscopy to quantify the percentage of cells exhibiting GFP–LC3 aggregation (% $GFP–LC3^{vac}$ cells, mean ± s.e.m., $n=3$, $^*P<0.05$).

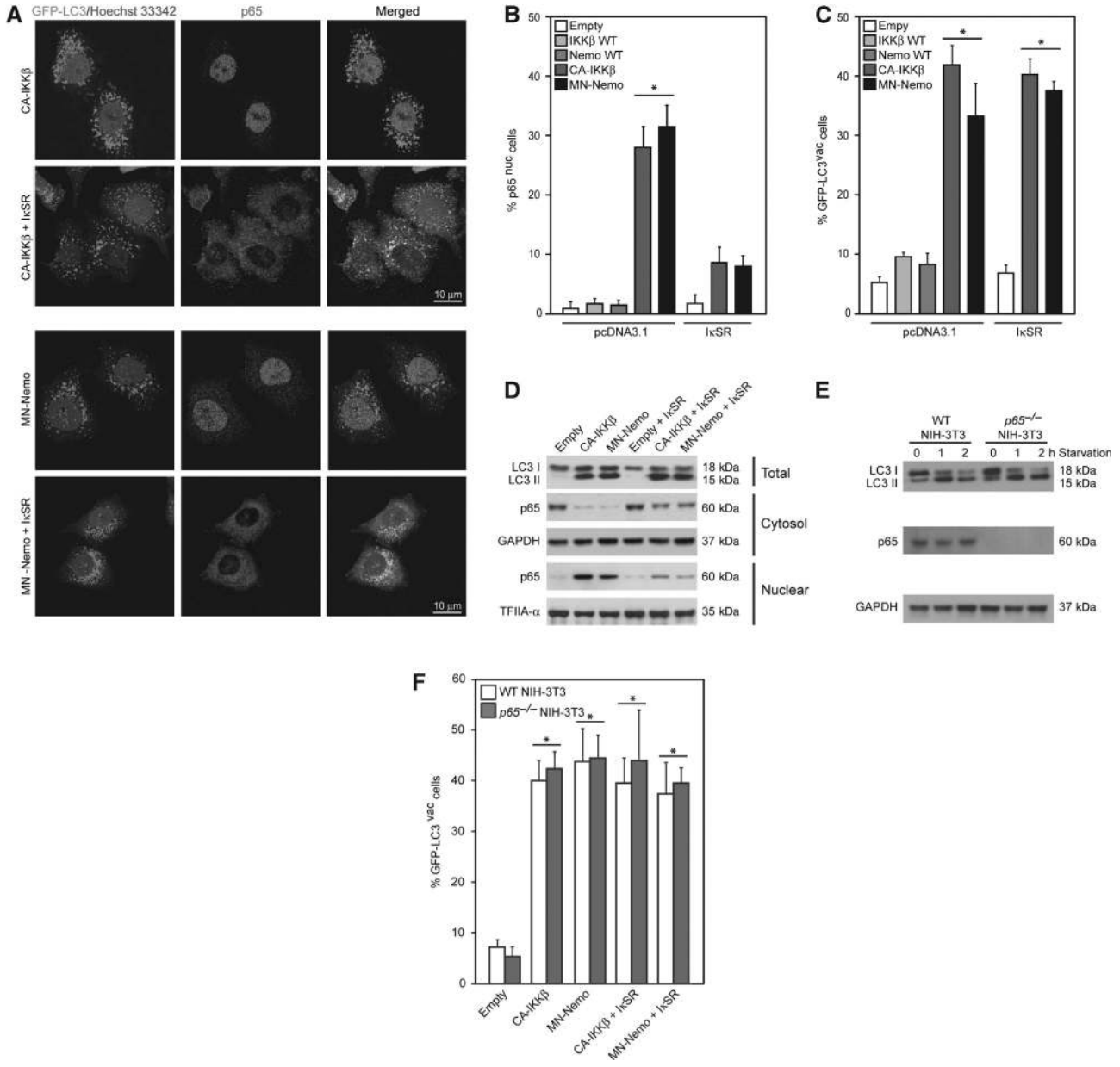

Figure 3 Autophagy induction by IKK can be uncoupled from NF-κB activation. (**A**–**C**) Effects of IκSR on NF-κB activation and autophagy induction by IKK, as determined by immunofluorescence microscopy. Cells were transfected simultaneously with a construct for the expression of GFP–LC3 plus the pcDNA3.1 vector or wild type (WT) IKKβ-, CA-IKKβ-, WT NEMO- or MN-NEMO-encoding plasmids alone or in combination with a plasmid that encodes IκSR, followed by immunofluorescence staining for the detection of p65. Representative microphotographs are shown in (**A**), whereas the percentage of transfected cells showing nuclear p65 translocation (% $p65^{nuc}$ cells) or cytoplasmic GFP–LC3 aggregation (% GFP-$LC3^{vac}$ cells) are shown in (**B**, **C**), respectively (mean ± s.e.m., $n=3$, $^*P<0.05$). (**D**) Effects of the IκB 'superrepressor' (IκSR) on NF-κB activation and autophagy induction by IKK, as assessed by immunoblotting. HeLa cells were transfected with the pcDNA3.1 vector or with WT IKKβ-, CA-IKKβ-, WT NEMO- or MN-NEMO-encoding plasmids alone or in association with a construct for the expression of IκSR for 18 h, followed by lysis and processing for immunoblotting determinations. The maturation of LC3 was assessed in whole-cell extracts. Alternatively, lysates were subjected to subcellular fractionation to evaluate the presence of p65/RelA in the cytoplasm versus the nucleus, using GAPDH and TFIIA-α to control equal loading of cytoplasmic and nuclear fractions, respectively. (**E**, **F**) Knockout of p65/RelA fails to affect autophagy. WT and $p65^{-/-}$ murine NIH-3T3 fibroblasts were exposed to starvation conditions for the indicated time, followed by immunoblotting assessment of LC3 maturation (**E**). Alternatively, cells were co-transfected with a GFP–LC3-encoding construct plus the pcDNA3.1 vector or the indicated IKK-relevant plasmids for 18 h, followed by immunofluorescence microscopy for the quantification of GFP–$LC3^{vac}$ cells (mean ± s.e.m., $n=3$, $^*P<0.05$) (**F**).

(Supplementary Figure S12), underscoring the absence of a strict correlation between autophagy induction and NF-κB activation *in vivo*. Notably, $IKK\beta^{\Delta hep}$ mice demonstrated a liver-specific defect in the starvation-induced depletion of p53 (Figure 6D), hypophosphorylation of $p70^{S6K}$ and hyperphosphorylation of AMPK and JNK1 (Figure 6E), supporting an intimate link between IKK and other regulators of autophagy. In conditions of starvation, we failed to detect a significant decrease in circulating glucose level in the context of the liver-specific autophagy defect (data not shown), similarly because other organs compensate this defect at the whole-body level.

Concluding remarks

In this report, we show that IKK effectively triggers autophagy and that optimal induction of autophagy by multiple stimuli requires IKK activation. However, the induction of autophagy did not correlate with NF-κB activation, and inhibition of NF-κB failed to prevent IKK-induced autophagy. By virtue of its kinase activity, IKK has multiple NF-κB-independent signalling functions (Hacker and Karin, 2006; Descargues *et al*, 2008), and autophagy apparently falls into the category of IKK-elicited responses that do not require NF-κB. At present, it is an open conundrum how IKK can be activated without leading to IκB degradation and hence NF-κB activation, as we have observed at least in some cell types (such as HeLa cells, Figure 1; and mouse splenocytes, Figure 5). As a speculative possibility, in such cells the level of IKK activation by autophagy inducers would be too low to lead to significant IκB phosphorylation and degradation, yet sufficiently high to participate in the induction of autophagy.

IκB kinase promotes autophagy through a canonical pathway involving p53 depletion, mTOR inhibition, AMPK and JNK1 activation, and release of the pro-autophagic protein Beclin-1 from its inhibitory interaction with Bcl-2. Several processes among these have been connected to each other in the past. Although AMPK might be a target of TAK1 (Herrero-Martin *et al*, 2009), there are no indications that AMPK would be a target of IKK. The NF-κB activation pathway and p53 are acting in multiple antagonistic pathways (Stoffel *et al*, 2004; Huang *et al*, 2007), and IKKβ can phosphorylate and destabilize p53 (Tergaonkar *et al*, 2002; Xia *et al*, 2009). Pharmacological inhibition of p53 with pifithrin-α (as well as the knockout of the *tp53* gene) reportedly suffices to activate IKK (Kawauchi *et al*, 2008), and activation of IKK can cause p53 depletion, as shown here, suggesting the existence of a self-amplifying regulatory circuit that may constitute a 'switch' for the rapid induction of autophagy in an all-or-nothing (rather than gradual) manner. Indeed, biological switches often involve such positive feed forward loops (Tapscott, 2005). AMPK is a negative regulator of mTOR (Sarbassov *et al*, 2005). Importantly, the inhibition of mTOR with rapamycin caused IKK activation, which in turn stimulated AMPK and inhibited mTOR, suggesting the existence of yet another self-amplifying circuit. Finally, JNK1 can phosphorylate the flexible loop of Bcl-2, thereby reducing its interaction with Beclin-1 and setting off the autophagic cascade (Wei *et al*, 2008). However, the mechanisms through which IKK activation favours that of JNK1 have not yet been elucidated, and several studies revealed that NF-κB (downstream of IKK) would actually inhibit JNK1 activation (Papa *et al*, 2006; Perkins, 2007).

Autophagy is a potent tumour-suppressive mechanism, presumably due to its essential contribution to the maintenance of genomic stability (Mathew *et al*, 2007), the avoidance of excessive ROS generation (Mathew *et al*, 2009) and its participation in cellular senescence (Young *et al*, 2009), which constitutes a barrier against oncogenesis. Accordingly, multiple genes that are required for the induction/execution of autophagy are potent tumour suppressors, including PTEN, TSC1, TSC2, LKB1, ATG4, Beclin-1, UVRAG, and BH3-only proteins of the Bcl-2 family (Maiuri *et al*, 2009). Here, we revealed the importance of the three components of the IKK complex for the autophagic process. Intriguingly, each of these IKK subunits has been shown to act as a tumour suppressor, in specific circumstances. The liver-specific knockout of NEMO causes hepatic carcinogenesis that is preceded by a type of hepatocellular steatosis (Luedde *et al*, 2007) that is reminiscent of that observed in *Beclin-1*$^{+/-}$ livers (Qu *et al*, 2003; Mathew *et al*, 2009). The liver-specific knockout of IKKβ enhances mutagen-induced hepatocarcinogenesis, in a process that is linked to inflammatory responses (Sakurai *et al*, 2006). Finally, the keratinocyte-specific knockout of IKKα facilitates the induction of squamous tumours in mice (Park *et al*, 2007), and inactivating IKKα mutations are frequently found in human skin cancers (Liu *et al*, 2006). Whether the tumour-suppressive function of IKK subunits can be explained by their contribution to autophagy remains an intriguing possibility for further investigation.

Materials and methods

Cell lines and culture conditions

Unless otherwise indicated, media and supplements for cell culture were purchased from Gibco-Invitrogen (Carlsbad, USA). All cell lines were cultured at 37°C under 5% CO_2, in medium containing 10% fetal calf serum (FCS) and 10 mM HEPES buffer. In addition, cell type-specific culture conditions include: Dulbecco's modified Eagle's medium (DMEM) + 1 mM sodium pyruvate for cervical carcinoma HeLa and osteosarcoma U2OS cells; DMEM/F12 medium + 100 U/ml penicillin G sodium and 100 μg/ml streptomycin sulfate for NSCLC A549 cells; DMEM + 1% non-essential amino acids (Sigma-Aldrich, St. Louis, USA) for WT, *map3k7*$^{-/-}$ (kind gift from S Akira, Osaka University), *chuk*$^{-/-}$, *ikbkb*$^{-/-}$, *ikbkg*$^{-/-}$ and *rela*$^{-/-}$ MEFs; DMEM for WT and *rela*$^{-/-}$ NIH-3T3 murine fibroblasts. For serum and amino-acid starvation, cells were cultured in serum-free Earle's Balanced Salt Solution (EBSS) medium (Sigma-Aldrich; Gonzalez-Polo *et al*, 2005). Metabolic stress was inflicted by culturing the cells for 48 h in EBSS medium under near-to-anoxic conditions (37°C, 0.1% oxygen, 5% CO_2).

Treatments and transfections

Cells were seeded in 6-, 12- or 24-well plates and allowed to attach for 12–24 h before the experiments. Cells were challenged for 0.5–12 h with the following pharmacological agents: 1 nM bafilomycin A1 (Sigma-Aldrich); 1 μM BAY11-7082 (BioMol, BioMol Research Laboratories, Plymouth Meeting, USA); 1 μM JNK inhibitor I (Calbiochem, San Diego, USA); 10 mM lithium chloride (Sigma-Aldrich); 10 μM nutlin-3 (Alexis Biochemicals, San Diego, USA); 30 μM pifithrin-α (Calbiochem); 1 μM rapamycin (Tocris Bioscience, Ellisville, USA); 10 μM RITA (Alexis Biochemicals); 10 μM SP600125 (Calbiochem); 1 ng/ml TNF-α (from Sigma-Aldrich); and 2.5 μM tunicamycin (Calbiochem). The siRNA transfection was performed using Oligofectamine® (Invitrogen), according to the manufacturer's instructions. Custom-designed siRNA duplexes targeting the following proteins were purchased from Sigma-Proligo: AMPKα (sense 5′-UGCCUACCAUCUCAUAAUAdTdT-3′); Beclin-1 (sense 5′-dTdT-3′; Gonzalez-Polo *et al*, 2005), IKKα (sense 5′-CAAAGAAGCU GACAAUACUdTdT-3′); IKKβ (sense 5′-GGAAGUACCUGAACCAGU UAdTdT-3′); MDM2 (sense 5′-AAGGAAUAAGCCCUGCCCAdTdT-3′); NEMO (sense 5′-AACAGGAGGUGAUCGAUAAdTdT-3′); p65/RelA (sense 5′-GGAUUGAGGAGAAACGUAA-3′); JNK1-1 (sense 5′-GGAA AGAAUUGAUAUAUAAdTdT-3′); c-Jun (sense 5′-GAACGUGACAGAU GAGCAGdTdT-3′); MKK4 (sense 5′-GGACGAGGAGCUUAUGGUUdT dT-3′); and MKK7 (sense 5′-AGAUGACAGUGGCGAUUGUdTdT-3′). The JNK1-2 siRNA was purchased from Santa Cruz Biotechnology (Santa Cruz, USA). An irrelevant siRNA duplex (sense 5′-GC CGGUAUGCCGGUUAAGUdTdT-3′) was used as a negative control. Plasmid transfection was carried out using Lipofectamine 2000® (Invitrogen), as recommended by the manufacturer. A plasmid encoding for the fusion protein GFP–LC3 (Kabeya *et al*, 2000) was co-transfected with the empty vector pcDNA3.1 (Invitrogen) or with plasmids overexpressing WT IKKβ, WT NEMO, dominant active IKKβ (CA-IKKβ; Mercurio *et al*, 1997) or a NEMO variant that

constitutively activates the IKK complex (MN-NEMO; Weil *et al*, 2003). Unless otherwise specified, cells were used 24 h after transfection.

Automated high content microscopy

A total of 10×10^3 U2OS cells stably co-expressing a green fluorescent protein (GFP)-LC3 chimera and histone 2B fused to red fluorescent protein (H2B-RFP) were seeded in 96-well imaging plates (BD Falcon, Sparks, USA) 24 h before treatment. The cells were washed with starvation medium and subsequently treated with the agents from the Institute of Chemistry and Cell Biology (ICCB, Harvard, USA) Known Bioactives Library (concentration range: 1–12 μM) re-suspended in starvation medium. At 12 h post-treatment, the cells were fixed with 4% paraformaldehyde (Sigma). Images were acquired using a BD pathway 855 automated microscope (BD Imaging Systems, San José, USA) equipped with a robotized Twister II plate handler (Caliper Life Sciences, Hopkinton, USA) using a $\times 20$ objective (Olympus, Center Valley, USA) and further analysed with BD Attovision software (BD Imaging Systems) for H2B–RFP-labelled nuclei and GFP–LC3 puncta in the cytoplasm. Doublets of images of approximately 250 cells for each compound treatment were analysed to obtain the cell number and the average cytosolic fluorescent spot number. The background levels of autophagy (in complete medium) was subtracted, and the effects of pharmacological inhibitors were calculated as percent inhibition of autophagy.

Cytofluorometry

The following fluorochromes were used to determine apoptosis-associated modifications: 3,3′-dihexyloxacarbocyanine iodide

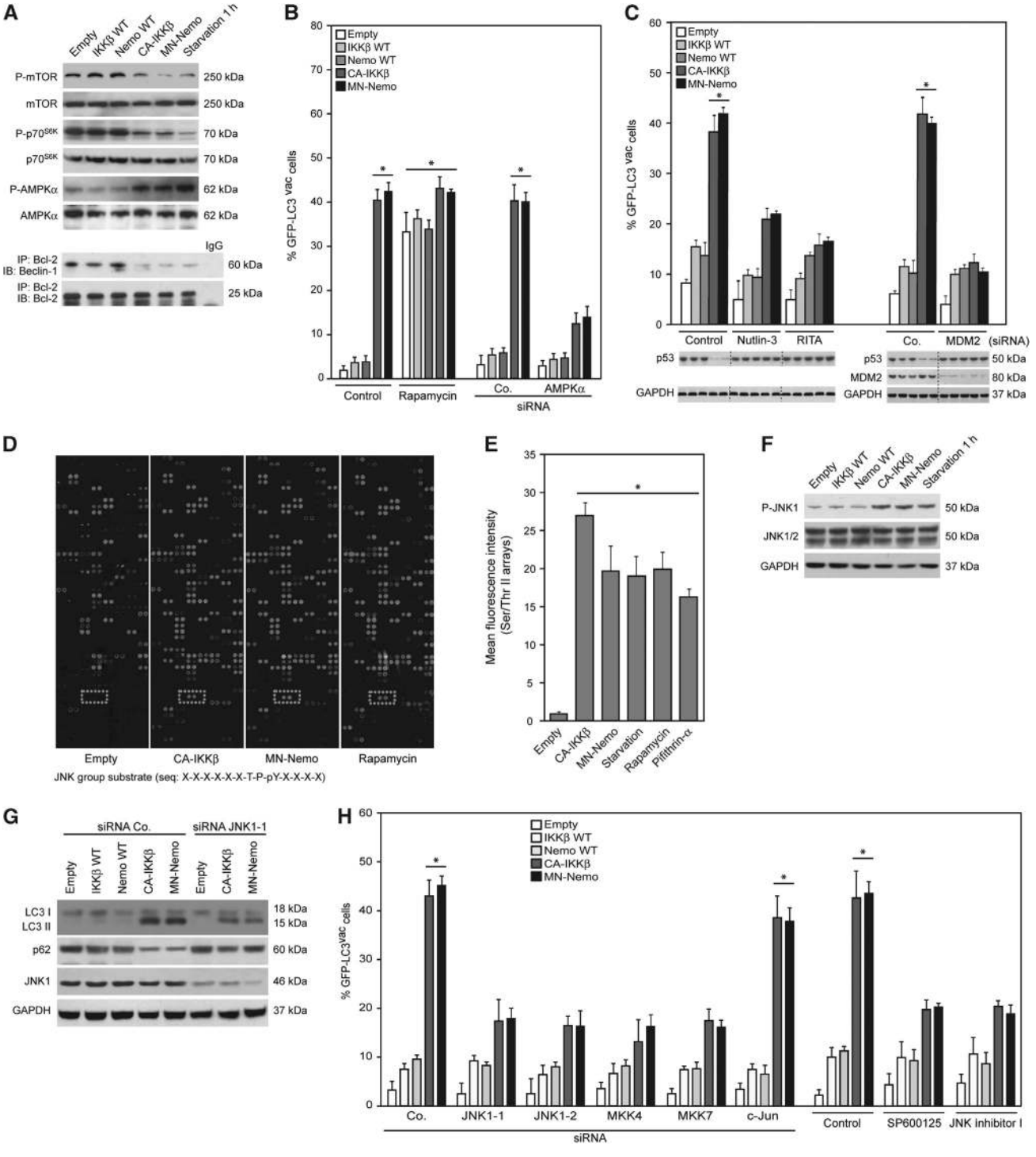

($DiOC_6(3)$, 40 nM; Molecular Probes-Invitrogen) for the quantification of the mitochondrial transmembrane potential ($\Delta\Psi_m$), and propidium iodide (PI, 1 μg/ml; Molecular Probes-Invitrogen) to determine cell viability (Gonzalez-Polo *et al*, 2005). On trypsinization, live cells were stained for 30 min at 37°C, followed by cytofluorometric analysis using a FACS Vantage (Becton Dickinson, San José, USA).

Immunoblotting and immunoprecipitation

For immunoblotting assessments, cells were washed with cold PBS at 4°C and lysed as previously described (Criollo *et al*, 2007). Fifty μg of proteins were separated according to molecular weight on 4–12% SDS–PAGE pre-cast gels (Invitrogen) and electrotransferred to Immobilon membranes (Millipore, Bedford, USA). Unspecific binding sites were blocked by incubating the membranes for 1 h in 0.05% Tween 20 (in TBS) supplemented with 5% w/v non-fat powdered milk. Primary antibodies specific for the following phospho- (P-) or total proteins were used: P-AMPK (Cell Signaling Technology, Beverly, USA); AMPKα (Cell Signaling Technology); Beclin-1 (Santa Cruz Biotechnology); Bcl-2 (Santa Cruz Biotechnology); c-Jun (Cell Signaling Technology); P-IκBα (Cell Signaling Technology); P-IKKα/β (Cell Signaling Technology); IKKα/β (Cell Signaling Technology); P-NEMO (Calbiochem); NEMO (Santa Cruz Biotechnology); LC3 (Cell Signaling Technology); P-mTOR (Cell Signaling Technology); MKK4 (Cell Signaling Technology), MKK7 (Cell Signaling Technology); mTOR (Santa Cruz Biotechnology); p53 (Santa Cruz Biotechnology); p62 (Santa Cruz Biotechnology); P-p70S6K (Cell Signaling Technology); p70S6K (Cell Signaling Technology); or TFIIAα (Santa Cruz Biotechnology). On overnight incubation at 4°C, primary antibodies were detected with the appropriate horseradish peroxidase-labelled secondary antibodies (Southern Biotechnologies Associates; Birmingham; UK) and the SuperSignal West Pico chemoluminescent substrate (Thermo Fisher Scientific, Rockford, USA). Primary antibodies that specifically recognize β-actin (Millipore) or GAPDH (Millipore) were used to ensure equal lane loading. For immunoprecipitation, 7×10^6 cells were lysed as previously described (Criollo *et al*, 2007), and 300 μg of proteins were pre-cleared for 1 h with 30 μl of Pure Proteome Protein G Magnetic Beads (Millipore), followed by incubation for 2 h in the presence of an anti-Bcl-2 antibody (Santa Cruz Biotechnology) or IgG control. Subsequent immunoblotting was carried out using TrueBlot-HRP (eBioscience, San Diego, USA) secondary antibodies.

Electrophoretic mobility shift assays (EMSA)

Nuclear extracts were prepared and analysed for DNA-binding activity using the HIV-LTR tandem κB oligonucleotide as a probe for NF-κB (Jacque *et al*, 2005). For supershift assays, nuclear extracts were pre-incubated with antibodies specific for p50/NFκB1 (Cell Signaling Technology); p52 (Cell Signaling Technology); p65/RelA (BD Bioscience); RelB (Cell Signaling Technology) or cRel (Santa Cruz Biotechnology) for 30 min on ice before the addition of the labelled probe.

IKK complex kinase assays

IκB kinase complexes were isolated from cell lysates by immunoprecipitation with an anti-NEMO antibody (BD Bioscience), and the associated kinase activity was determined with 2 μg of the semi-synthetic IκBα-derived IKK substrate GST–IκBα (1–54), as previously described (Hu *et al*, 1999). The amount of IKKβ was determined by immunoblotting.

Kinome analyses

Cells were collected, washed in cold PBS, re-suspended in 200 μl lysis buffer, gently homogenized and kept in ice bath for 10 min. Thereafter, lysates were centrifuged at 10 000 r.p.m. (4°C, 20 min) to remove debris, and protein concentration in the supernatants was determined by means of the DC protein assay (BioRad Laboratories, Hercules, USA). A total of 200 μg of proteins was then incubated for 30 min at room temperature (RT) on top of Intavis CelluSpot® Serine/Threonine-kinase substrate microarrays, in kinase buffer (Cell Signaling Technology) supplemented with 1% bovine serum albumin (BSA). On washing, microarrays were incubated for 45 min with a cocktail of two biotin-conjugated antibodies that specifically recognize serine and threonine phosphoresidues (Sigma-Adrich). Finally, arrays were incubated with AlexaFluor® 647–streptavidin conjugates (Molecular Probes-Invitrogen) for 45 min before fluorescence measurement using a GenePix® 4000B microarray scanner (Molecular Devices, Sunnyvale, USA).

Animal and tissue processing

All animals were bred and maintained according to both the FELASA and the Animal Experimental Ethics Committee Guidelines (Val de Marne, France). C57BL/6 mice were obtained from Charles River Laboratory, France, and ALB Cre IKK F/F mice (UCSD Docket No. SD2004-120; Oakland, California) were provided by Urszula Hibner and Michael Karin. Mice were housed in a temperature-controlled environment with 12 h light/dark cycles and received food and water *ad libitum*. For starvation studies, mice were deprived of food for 24 h but had free access to drinking water. Alternatively, mice were injected i.p. with 5 mg/kg rapamycin 24 h before killing. Mice were anesthetized and killed according to the FELASA guidelines. The liver, pancreas, heart, spleen and kidneys were collected and fixed with 4% paraformaldehyde for at least 4 h, followed by overnight treatment with 30% saccharose in PBS, at 4°C. Tissue biopsies were finally embedded in Tissue-Tek OCT

Figure 4 Implication of AMPK, mTOR, p53 and JNK1 in autophagy induction by IKK activation. (**A**) Activation of AMPK, inhibition of mTOR and dissociation of the Beclin-1–Bcl-2 complex in response to IKK activation. HeLa cells were subjected to starvation conditions for 1 h or transfected with the pcDNA3.1 vector or wild type (WT) IKKβ-, CA-IKKβ-, WT NEMO- or MN-NEMO-encoding plasmids for 18 h, followed by immunoblotting detection of the indicated proteins. Alternatively, lysates were immunoprecipitated with a Beclin-1-specific antibody and then subjected to immunoblotting detection of Beclin-1 or Bcl-2. (**B**) Involvement of AMPK and mTOR in IKK-induced autophagy. Before transfection with a GFP–LC3-encoding construct plus the indicated plasmids for 12 h, HeLa cells were transfected for 48 h with a control siRNA (Co.) or an AMPKα-specific siRNA. Alternatively, 12 h after plasmid transfection alone, cells were treated with rapamycin or with an equivalent volume of DMSO (solvent control) for 6 h. Columns depict the percentage of cells exhibiting GFP–LC3 aggregation (% GFP–$LC3^{vac}$ cells, mean ± s.e.m., $n=3$, $^*P<0.05$). (**C**) Involvement of p53 degradation in IKK-induced autophagy. MEFs were transfected with a control (Co.) or an MDM2-specific siRNA for 24 h, then transfected again with a plasmid encoding GFP–LC3 construct plus the indicated constructs for 6 h. As an alternative, 6 h after plasmid transfection alone cells were treated with Nutlin-3 or RITA for additional 12 h. Finally, cells were subjected to immunofluorescence microscopy for the quantification of GFP–LC3 aggregation. Columns report the % of GFP–$LC3^{vac}$ cells (mean ± s.e.m., $n=3$, $^*P<0.05$). (**D**, **E**) Kinome analysis for the detection of serine/threonine kinase substrates phosphorylation triggered by autophagic stimuli. CelluSpot serine/threonine-kinase substrate microarrays were incubated for with extracts from cells that were transfected with the pcDNA3.1 vector or with CA-IKKβ- or MN-NEMO-encoding plasmids for 18 h. As an alternative, extracts were obtained from cells subjected to starvation conditions or treated with rapamycin or pifithrin-α for 2 h. Phosphorylation was revealed by means of fluorescence-labelled anti-phosphoserine/threonine antibodies. The dotted line in (**D**) highlights the position of a synthetic JNK1 substrate which is phosphorylated by extracts from cells undergoing autophagy. Panel (**E**) depicts the fold-induction of this signal (mean ± s.e.m., $n=2$, $^*P<0.05$). (**F**) CA-IKKβ and MN-NEMO induce JNK1 phosphorylation. Extracts from HeLa cells transfected or treated as in (**A**) were subjected to immunoblotting detection of phosphorylated (P-) and total JNK1. GAPDH levels were monitored to ensure equal loading. (**G**, **H**) Effect of JNK1 depletion/inhibition on IKK-induced autophagy. Cells were transfected with a control (Co.) or a JNK1-specific siRNA for 24 h, followed by transfection with the indicated constructs for additional 12 h and immunoblotting assessment of the maturation of LC3 and of the depletion of p62 (**G**). Cells were left untreated or transfected with the indicated siRNAs for 24 h, followed by further transfection with a construct encoding GFP–LC3 plus the indicated plasmids for 12 h. Alternatively, cell were pre-treated for 30 min with the indicated JNK1 inhibitors (or with an equal volume of DMSO) and then co-transfected with a GFP–LC3-encoding construct plus the indicated plasmids for additional 12 h (**H**). Columns depict the % of GFP–$LC3^{vac}$ cells (mean ± s.e.m., $n=3$, $^*P<0.05$).

compound (Sakura Finetek Europe B.V., Zoeterwoude, The Netherlands) and stored at −20°C.

Confocal microscopy of tissue sections

To examine LC3 distribution, 10 μm-thick cryosections were rinsed with PBS, permeabilized for 10 min with 0.3% Triton-X 100, saturated for 30 min with 5% BSA and incubated overnight with a primary anti-APG8b antibody (Abgent, San Diego, USA). Sections were then rinsed with PBS, incubated for 1 h at RT with an AlexaFluor® 488-conjugated secondary antibody (Molecular Probes-Invitrogen), post-fixed twice for 10 min with 4% paraformaldehyde (w/v in PBS), stained for 15 min with 10 μg/ml Hoechst

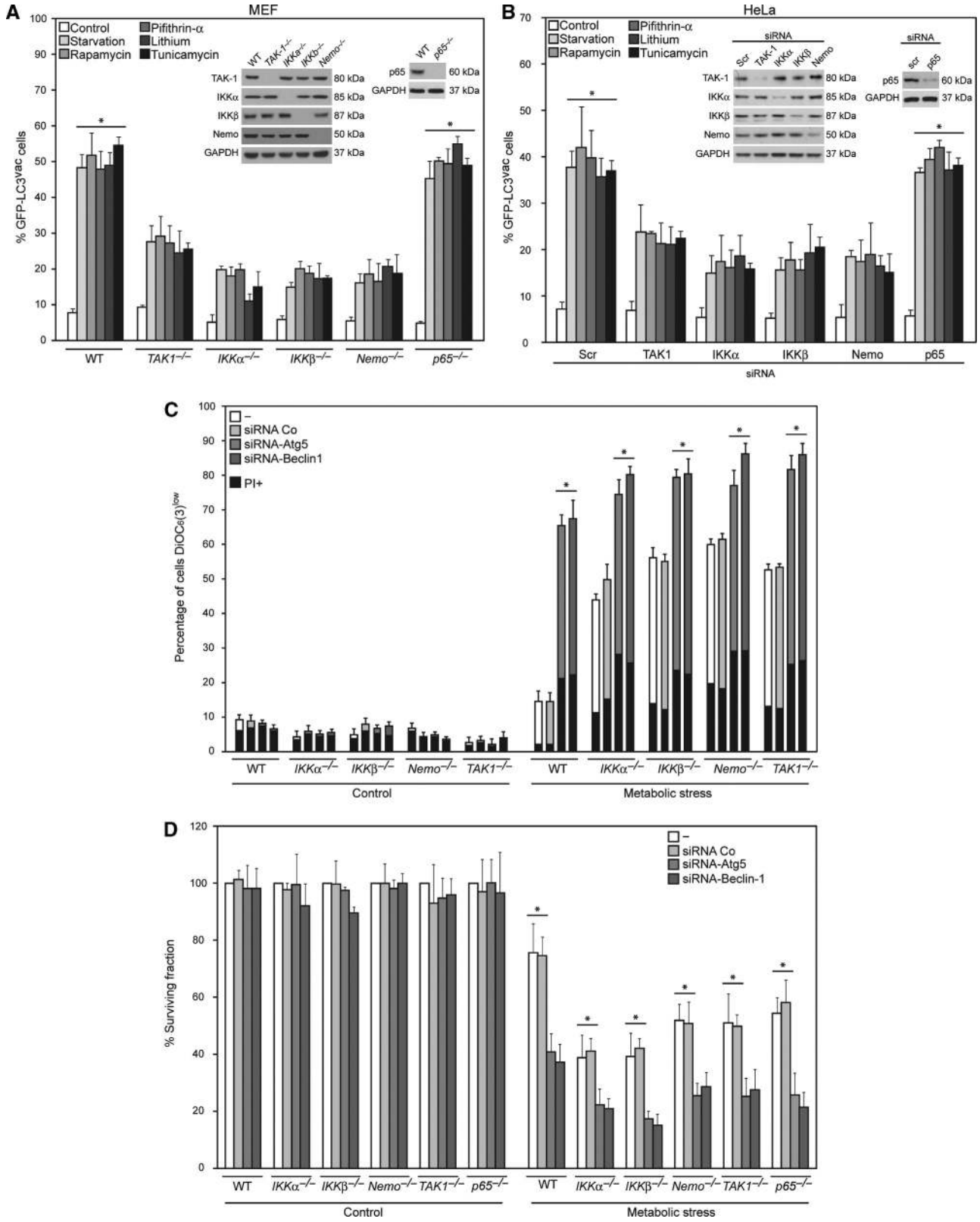

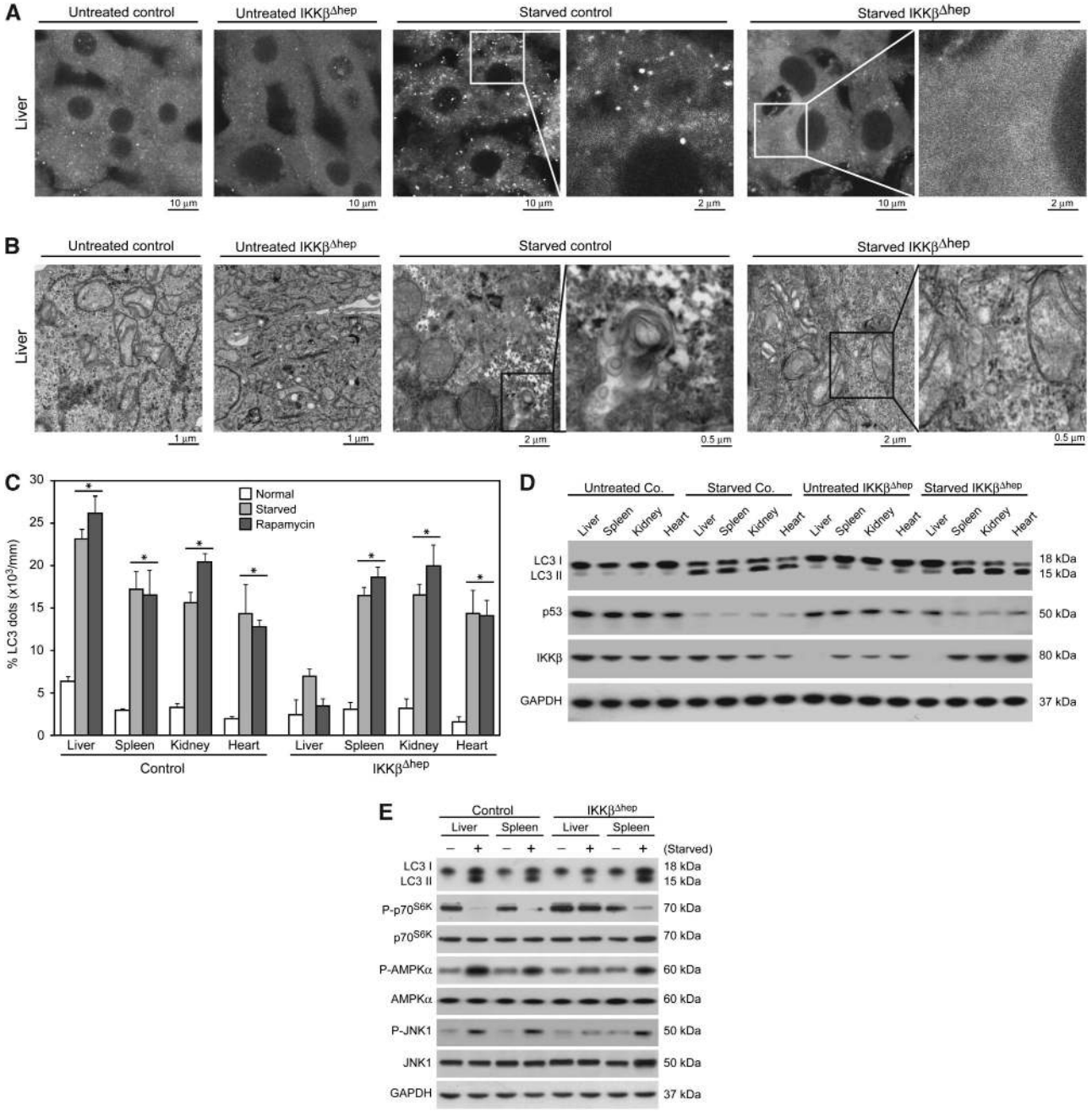

Figure 6 Implication of the IKK complex in the induction of autophagy *in vivo*. (**A**–**D**) Mice with the indicated genotype were subjected to food deprivation for 24 h or injected i.p. with rapamycin, followed by necropsy. Livers (**A**, **C**) and other organs (**C**) were subjected to the immunohistochemical detection of LC3 dots in the cytoplasm of parenchymatous cells. Columns illustrate the number of LC3 dots per mm^2 (mean ± s.e.m., $n = 3$, $^*P < 0.05$) (**C**). Alternatively, tissue sections were analysed by transmission electron microscopy for the detection of autophagosomes and autolysosomes (**B**), and parenchimal cells were processed for the detection of LC3 maturation, p53 and IKKβ (**D**). (**E**) Blockade of upstream autophagic signals in IKKβ-deficient hepatocytes. Livers and spleens from control or IKKβ$^{\Delta hep}$ mice that had been housed or not in starvation conditions for 24 h were processed for the immunoblotting assessment of the indicated proteins. Results are representative of three independent determinations.

Figure 5 Implication and functional impact of the IKK complex in the induction of autophagy *in vitro*. (**A**, **B**) Contribution of IKK subunits to autophagy in cultured cells. MEFs with the indicated genotype were transfected for 12 h with a GFP–LC3-encoding plasmid, cultured for 4 h in the presence of the indicated autophagy inducers, and eventually analysed by immunofluorescence microscopy for GFP–LC3 puncta. (**B**) Alternatively, HeLa cells were transfected with a control siRNA (Co.) or with siRNAs targeting the indicated proteins for 24 h, followed by transfection with the GFP–LC3-encoding plasmid, autophagy induction and immunofluorescence microscopy as in (**A**). In (**A**, **B**), columns depict the percentage of cells exhibiting GFP–LC3 in cytoplasmic dots (% GFP–LC3^{vac} cells, mean ± s.e.m., $n = 3$, $^*P < 0.05$), whereas inserts illustrate the efficacy of knockout or knockdown, as assessed by immunoblotting. (**C**, **D**) Impact of IKK constituents and autophagy-relevant proteins on cell viability in conditions of autophagy induction and metabolic stress. (**C**) MEFs of the indicated genotype were transfected for 24 h with a control siRNA (Co.) or with siRNAs targeting the indicated autophagy-relevant proteins, then subjected to metabolic stress (glucose deprivation, 0.1% oxygen) for 48 h and stained for cytofluorometric determination of apoptosis-associated parameters. Black and white or grey columns illustrate the percentage of cells (mean ± s.e.m., $n = 3$, $^*P < 0.05$) characterized by plasma membrane breakdown (PI$^+$) or loss of $\Delta\Psi_m$ (DiOC$_6$(3)^{low}/PI$^-$), respectively. (**D**) MEFs characterized by the indicated genetic deficiency were subjected to metabolic stress and plated to determine clonogenic survival. Column depict mean clonogenic survival ± s.e.m. ($n = 3$, $^*P < 0.05$).

33342, post-fixed once more with the same fixative and finally mounted. Immunofluorescence images were taken with a TCS SPE confocal microscope (Leica Microsystems, Weitzler, USA) and analysed with the Leica Suite Advanced Fluorescence software.

Light and immunofluorescence microscopy

Cells were processed for immunofluorescence staining according to established protocols (Criollo *et al*, 2007). Fixed and permeabilized cells were then stained with primary antibodies that recognize Lamp2 (Santa Cruz Biotechnology), p62 (Santa Cruz Biotechnology) or p65 (Santa Cruz Biotechnology), which were revealed with the appropriate AlexaFluor® conjugates (Molecular Probes). Nuclei were counterstained with 10 μg/ml Hoechst 33342 (Molecular Probes-Invitrogen). Fluorescence and confocal fluorescence microscopy assessments were performed using an IRE2 microscope (Leica Microsystems) equipped with a DC300F camera and with an LSM 510 microscope (Carl Zeiss, Jena, Germany), respectively. To determine the percentage of co-localization, Image J software was used.

Electron microscopy

Cells were fixed for 1 h at 4°C in 1.6% glutaraldehyde in 0.1 M Sörensen phosphate buffer (pH 7.3), washed, fixed again in aqueous 2% osmium tetroxide, stained in 2% uranyl acetate in 30% methanol and finally embedded in Epon. Electron microscopy was performed with a Tecnai G2 Spirit electron microscope (FEI, Eindhoven, The Netherlands), at 80 kV, on ultrathin sections (80 nm) stained with lead citrate and uranyl acetate.

Statistical procedures

Unless otherwise indicated, experiments were performed in triplicate and repeated at least twice. Figures show the results from one representative experiment (mean ± s.e.m., $n = 3$ parallel samples). Data were analysed using Microsoft Excel (Microsoft, Redmond, USA) and statistical significance was assessed by means of two-tailed Student's *t*-test ($^*P < 0.05$).

Supplementary data

Supplementary data are available at *The EMBO Journal* Online (http://www.embojournal.org).

Acknowledgements

We are indebted to Michael Karin (University of Californa, San Diego, USA), for the gift of knockout mice. We acknowledge the contribution of Sandra Güemes (Instituto de Biologia y Genetica Molecular, IBGM, Valladolid, Spain) for technical support. $p65^{-/-}$ MEFs were kindly provided by Thomas Meyer (Max Planck Institute, Berlin). GK is supported by the Ligue Nationale contre le Cancer (Equipe labellisée), Agence Nationale de la Recherche, Cancéropôle Ile-de-France, Institut National du Cancer, European Commission (Active p53, Apo-Sys, RIGHT, TransDeath, ChemoRes, ApopTrain), and Fondation pour la Recherche Médicale (FRM). We thank the International Collaboration Program ECOS-CONICYT, grant C08S01 (to GK and SL). EM is supported by the ApopTrain Marie Curie training network of the European Union. VB is supported by Agence Nationale pour la Recherche, Association pour la Recherche sur le Cancer, Belgian InterUniversity Attraction Pole, Cancéropole Ile-de-France, Institut National du Cancer, and Université Paris Descartes. OK is supported by EMBO, LG by Apo-Sys.

Conflict of interest

The authors declare that they have no conflict of interest.

References

Anckar J, Sistonen L (2007) Heat shock factor 1 as a coordinator of stress and developmental pathways. *Adv Exp Med Biol* **594:** 78–88

Anderson P, Kedersha N (2008) Stress granules: the Tao of RNA triage. *Trends Biochem Sci* **33:** 141–150

Arkan MC, Hevener AL, Greten FR, Maeda S, Li ZW, Long JM, Wynshaw-Boris A, Poli G, Olefsky J, Karin M (2005) IKK-beta links inflammation to obesity-induced insulin resistance. *Nat Med* **11:** 191–198

Baud V, Karin M (2009) Is NF-kappaB a good target for cancer therapy? Hopes and pitfalls. *Nat Rev Drug Discov* **8:** 33–40

Broemer M, Krappmann D, Scheidereit C (2004) Requirement of Hsp90 activity for IkappaB kinase (IKK) biosynthesis and for constitutive and inducible IKK and NF-kappaB activation. *Oncogene* **23:** 5378–5386

Budanov AV, Karin M (2008) p53 target genes sestrin1 and sestrin2 connect genotoxic stress and mTOR signaling. *Cell* **134:** 451–460

Copetti T, Bertoli C, Dalla E, Demarchi F, Schneider C (2009) p65/RelA modulates BECN1 transcription and autophagy. *Mol Cell Biol* **29:** 2594–2608

Crighton D, Wilkinson S, O'Prey J, Syed N, Smith P, Harrison PR, Gasco M, Garrone O, Crook T, Ryan KM (2006) DRAM, a p53-induced modulator of autophagy, is critical for apoptosis. *Cell* **126:** 121–134

Criollo A, Maiuri MC, Tasdemir E, Vitale I, Fiebig AA, Andrews D, Molgo J, Diaz J, Lavandero S, Harper F, Pierron G, di Stefano D, Rizzuto R, Szabadkai G, Kroemer G (2007) Regulation of autophagy by the inositol trisphosphate receptor. *Cell Death Differ* **14:** 1029–1039

Dan HC, Baldwin AS (2008) Differential involvement of IkappaB kinases alpha and beta in cytokine- and insulin-induced mammalian target of rapamycin activation determined by Akt. *J Immunol* **180:** 7582–7589

Descargues P, Sil AK, Karin M (2008) IKKalpha, a critical regulator of epidermal differentiation and a suppressor of skin cancer. *EMBO J* **27:** 2639–2647

DiDonato JA, Mercurio F, Karin M (1995) Phosphorylation of I kappa B alpha precedes but is not sufficient for its dissociation from NF-kappa B. *Mol Cell Biol* **15:** 1302–1311

Djavaheri-Mergny M, Amelotti M, Mathieu J, Besancon F, Bauvy C, Souquere S, Pierron G, Codogno P (2006) NF-kappaB activation represses tumor necrosis factor-alpha-induced autophagy. *J Biol Chem* **281:** 30373–30382

Duran A, Linares JF, Galvez AS, Wikenheiser K, Flores JM, Diaz-Meco MT, Moscat J (2008) The signaling adaptor p62 is an important NF-kappaB mediator in tumorigenesis. *Cancer Cell* **13:** 343–354

Gonzalez-Polo RA, Boya P, Pauleau AL, Jalil A, Larochette N, Souquere S, Eskelinen EL, Pierron G, Saftig P, Kroemer G (2005) The apoptosis/autophagy paradox: autophagic vacuolization before apoptotic death. *J Cell Sci* **118:** 3091–3102

Hacker H, Karin M (2006) Regulation and function of IKK and IKK-related kinases. *Sci STKE* **2006:** re13

Herrero-Martin G, Hoyer-Hansen M, Garcia-Garcia C, Fumarola C, Farkas T, Lopez-Rivas A, Jaattela M (2009) TAK1 activates AMPK-dependent cytoprotective autophagy in TRAIL-treated epithelial cells. *EMBO J* **28:** 677–685

Hu Y, Baud V, Delhase M, Zhang P, Deerinck T, Ellisman M, Johnson R, Karin M (1999) Abnormal morphogenesis but intact IKK activation in mice lacking the IKKalpha subunit of IkappaB kinase. *Science* **284:** 316–320

Huang WC, Ju TK, Hung MC, Chen CC (2007) Phosphorylation of CBP by IKKalpha promotes cell growth by switching the binding preference of CBP from p53 to NF-kappaB. *Mol Cell* **26:** 75–87

Jacque E, Tchenio T, Piton G, Romeo PH, Baud V (2005) RelA repression of RelB activity induces selective gene activation downstream of TNF receptors. *Proc Natl Acad Sci USA* **102:** 14635–14640

Kabeya Y, Mizushima N, Ueno T, Yamamoto A, Kirisako T, Noda T, Kominami E, Ohsumi Y, Yoshimori T (2000) LC3, a mammalian homologue of yeast Apg8p, is localized in autophagosome membranes after processing. *EMBO J* **19:** 5720–5728

Kawauchi K, Araki K, Tobiume K, Tanaka N (2008) p53 regulates glucose metabolism through an IKK-NF-kappaB pathway and inhibits cell transformation. *Nat Cell Biol* **10:** 611–618

Kedersha N, Chen S, Gilks N, Li W, Miller IJ, Stahl J, Anderson P (2002) Evidence that ternary complex (eIF2-GTP-tRNA(i)(Met))-deficient preinitiation complexes are core constituents of mammalian stress granules. *Mol Biol Cell* **13:** 195–210

Klionsky DJ (2004) Cell biology: regulated self-cannibalism. *Nature* **431:** 31–32

Klionsky DJ, Abeliovich H, Agostinis P, Agrawal DK, Aliev G, Askew DS, Baba M, Baehrecke EH, Bahr BA, Ballabio A, Bamber BA, Bassham DC, Bergamini E, Bi X, Biard-Piechaczyk M, Blum JS, Bredesen DE, Brodsky JL, Brumell JH, Brunk UT *et al* (2008) Guidelines for the use and interpretation of assays for monitoring autophagy in higher eukaryotes. *Autophagy* **4:** 151–175

Lawler S, Fleming Y, Goedert M, Cohen P (1998) Synergistic activation of SAPK1/JNK1 by two MAP kinase kinases *in vitro*. *Curr Biol* **8:** 1387–1390

Lee DF, Kuo HP, Chen CT, Hsu JM, Chou CK, Wei Y, Sun HL, Li LY, Ping B, Huang WC, He X, Hung JY, Lai CC, Ding Q, Su JL, Yang JY, Sahin AA, Hortobagyi GN, Tsai FJ, Tsai CH *et al* (2007) IKK beta suppression of TSC1 links inflammation and tumor angiogenesis via the mTOR pathway. *Cell* **130:** 440–455

Levine B, Kroemer G (2008) Autophagy in the pathogenesis of disease. *Cell* **132:** 27–42

Liu B, Park E, Zhu F, Bustos T, Liu J, Shen J, Fischer SM, Hu Y (2006) A critical role for I kappaB kinase alpha in the development of human and mouse squamous cell carcinomas. *Proc Natl Acad Sci USA* **103:** 17202–17207

Luedde T, Beraza N, Kotsikoris V, van Loo G, Nenci A, De Vos R, Roskams T, Trautwein C, Pasparakis M (2007) Deletion of NEMO/IKKgamma in liver parenchymal cells causes steatohepatitis and hepatocellular carcinoma. *Cancer Cell* **11:** 119–132

Maiuri MC, Tasdemir E, Criollo A, Morselli E, Vicencio JM, Carnuccio R, Kroemer G (2009) Control of autophagy by oncogenes and tumor suppressor genes. *Cell Death Differ* **16:** 87–93

Martin P, Diaz-Meco MT, Moscat J (2006) The signaling adapter p62 is an important mediator of T helper 2 cell function and allergic airway inflammation. *EMBO J* **25:** 3524–3533

Mathew R, Karantza-Wadsworth V, White E (2007) Role of autophagy in cancer. *Nat Rev Cancer* **7:** 961–967

Mathew R, Karp C, Beaudoin B, Vuong N, Chen G, Chen J-Y, Bray K, Reddy A, Bhanot G, Gelinas G, DiPaola RS, Karantza-Wadsworth V, White E (2009) Autophagy suppresses tumorigenesis through elimination of p62. *Cell* **137:** 1062–1075

Meley D, Bauvy C, Houben-Weerts JH, Dubbelhuis PF, Helmond MT, Codogno P, Meijer AJ (2006) AMP-activated protein kinase and the regulation of autophagic proteolysis. *J Biol Chem* **281:** 34870–34879

Mercurio F, Zhu H, Murray BW, Shevchenko A, Bennett BL, Li J, Young DB, Barbosa M, Mann M, Manning A, Rao A (1997) IKK-1 and IKK-2: cytokine-activated IkappaB kinases essential for NF-kappaB activation. *Science* **278:** 860–866

Mizushima N, Klionsky DJ (2007) Protein turnover via autophagy: implications for metabolism. *Annu Rev Nutr* **27:** 19–40

Papa S, Bubici C, Zazzeroni F, Pham CG, Kuntzen C, Knabb JR, Dean K, Franzoso G (2006) The NF-kappaB-mediated control of the JNK cascade in the antagonism of programmed cell death in health and disease. *Cell Death Differ* **13:** 712–729

Papandreou I, Lim AL, Laderoute K, Denko NC (2008) Hypoxia signals autophagy in tumor cells via AMPK activity, independent of HIF-1, BNIP3, and BNIP3L. *Cell Death Differ* **15:** 1572–1581

Park E, Zhu F, Liu B, Xia X, Shen J, Bustos T, Fischer SM, Hu Y (2007) Reduction in IkappaB kinase alpha expression promotes the development of skin papillomas and carcinomas. *Cancer Res* **67:** 9158–9168

Pattingre S, Tassa A, Qu X, Garuti R, Liang XH, Mizushima N, Packer M, Schneider MD, Levine B (2005) Bcl-2 antiapoptotic proteins inhibit Beclin-1-dependent autophagy. *Cell* **122:** 927–939

Perkins ND (2007) Integrating cell-signalling pathways with NF-kappaB and IKK function. *Nat Rev Mol Cell Biol* **8:** 49–62

Qing G, Yan P, Qu Z, Liu H, Xiao G (2007) Hsp90 regulates processing of NF-kappa B2 p100 involving protection of NF-kappa B-inducing kinase (NIK) from autophagy-mediated degradation. *Cell Res* **17:** 520–530

Qu X, Yu J, Bhagat G, Furuya N, Hibshoosh H, Troxel A, Rosen J, Eskelinen EL, Mizushima N, Ohsumi Y, Cattoretti G, Levine B (2003) Promotion of tumorigenesis by heterozygous disruption of the Beclin-1 autophagy gene. *J Clin Invest* **112:** 1809–1820

Riley T, Sontag E, Chen P, Levine A (2008) Transcriptional control of human p53-regulated genes. *Nat Rev Mol Cell Biol* **9:** 402–412

Sakurai T, Maeda S, Chang L, Karin M (2006) Loss of hepatic NF-kappa B activity enhances chemical hepatocarcinogenesis through sustained c-Jun N-terminal kinase 1 activation. *Proc Natl Acad Sci USA* **103:** 10544–10551

Sarbassov DD, Ali SM, Sabatini DM (2005) Growing roles for the mTOR pathway. *Curr Opin Cell Biol* **17:** 596–603

Schlottmann S, Buback F, Stahl B, Meierhenrich R, Walter P, Georgieff M, Senftleben U (2008) Prolonged classical NF-kappaB activation prevents autophagy upon E. coli stimulation *in vitro*: a potential resolving mechanism of inflammation. *Mediators Inflamm* **2008:** 725854

Semenza GL (2007) Hypoxia-inducible factor 1 (HIF-1) pathway. *Sci STKE* **2007:** cm8

Stoffel A, Chaurushiya M, Singh B, Levine AJ (2004) Activation of NF-kappaB and inhibition of p53-mediated apoptosis by API2/mucosa-associated lymphoid tissue 1 fusions promote oncogenesis. *Proc Natl Acad Sci USA* **101:** 9079–9084

Talloczy Z, Jiang W, Virgin HW 4th, Leib DA, Scheuner D, Kaufman RJ, Eskelinen EL, Levine B (2002) Regulation of starvation- and virus-induced autophagy by the eIF2alpha kinase signaling pathway. *Proc Natl Acad Sci USA* **99:** 190–195

Tapscott SJ (2005) The circuitry of a master switch: Myod and the regulation of skeletal muscle gene transcription. *Development* **132:** 2685–2695

Tasdemir E, Maiuri MC, Galluzzi L, Vitale I, Djavaheri-Mergny M, D'Amelio M, Criollo A, Morselli E, Zhu C, Harper F, Nannmark U, Samara C, Pinton P, Vicencio JM, Carnuccio R, Moll UM, Madeo F, Paterlini-Brechot P, Rizzuto R, Szabadkai G *et al* (2008) Regulation of autophagy by cytoplasmic p53. *Nat Cell Biol* **10:** 676–687

Tergaonkar V, Pando M, Vafa O, Wahl G, Verma I (2002) p53 stabilization is decreased upon NFkappaB activation: a role for NFkappaB in acquisition of resistance to chemotherapy. *Cancer Cell* **1:** 493–503

Vallabhapurapu S, Karin M (2009) Regulation and function of NF-kappaB transcription factors in the immune system. *Annu Rev Immunol* **27:** 693–733

Wei Y, Pattingre S, Sinha S, Bassik M, Levine B (2008) JNK1-mediated phosphorylation of Bcl-2 regulates starvation-induced autophagy. *Mol Cell* **30:** 678–688

Weil R, Schwamborn K, Alcover A, Bessia C, Di Bartolo V, Israel A (2003) Induction of the NF-kappaB cascade by recruitment of the scaffold molecule NEMO to the T cell receptor. *Immunity* **18:** 13–26

Xia Y, Padre RC, De Mendoza TH, Bottero V, Tergaonkar VB, Verma IM (2009) Phosphorylation of p53 by IkappaB kinase 2 promotes its degradation by beta-TrCP. *Proc Natl Acad Sci USA* **106:** 2629–2634

Young AR, Narita M, Ferreira M, Kirschner K, Sadaie M, Darot JF, Tavare S, Arakawa S, Shimizu S, Watt FM, Narita M (2009) Autophagy mediates the mitotic senescence transition. *Genes Dev* **23:** 798–803

Zhang H, Bosch-Marce M, Shimoda LA, Tan YS, Baek JH, Wesley JB, Gonzalez FJ, Semenza GL (2008) Mitochondrial autophagy is an HIF-1-dependent adaptive metabolic response to hypoxia. *J Biol Chem* **283:** 10892–10903